Sea level controls on the geomorphic evolution of Geographe Bay, south-west Australia

GIADA BUFARALE [1*], MICHAEL J O'LEARY [2] & JULIEN BOURGET [2]

[1] *Department of Applied Geology, Curtin University, GPO Box U1987, Perth, WA 6845, Australia*

[2] *School of Earth Sciences, University of Western Australia, Crawley, WA 6009, Australia*

* *Corresponding author:* ✉ *giada.bufarale@postgrad.curtin.edu.au*

Abstract

High-resolution shallow seismic profiles collected along the inner shelf in Geographe Bay (south-west Australia) illustrate a highly-variable buried architecture. Three main acoustic units, separated by unconformities, correspond to different geological facies, deposited under various sea-level conditions. The acoustic basement (Unit B) belongs to the Lower Cretaceous Leederville Formation; the middle unit is attributable to the Tamala Limestone (Unit P, Mid- to Late Pleistocene) and the top unit (Unit H) is Holocene. Combining the seismic data with high-resolution bathymetry and sediment grabs, several surficial and buried morphological features are revealed, including sandbars, palaeochannels and ridges.

The shore-oblique sandbars have been directly influenced by local hydrodynamics including mean wave direction and currents, benthic habitats such as seagrass, and sediment grain size. The palaeochannels (buried and surficial) are the expression of previous sea-level lowstands. Two sets of shore-parallel, low-relief ridges, at depths of ~7 m and ~20 m, are relict landforms that are most likely regressive beach ridges and sub-littoral deposits, belonging to the Tamala Limestone. These structures were formed during Late Pleistocene relatively high sea-level stages (late Marine Isotope Stages 5e and 5c, respectively, between 120 and 100 thousand years ago), cemented when the sea level was lower and subsequently subject to transgressive erosion.

The newly acquired seismic datasets shows that the inner shelf is mostly covered by a veneer of sediment (with average thickness of 50 cm) above the Pleistocene hard surface, whereas sandbars can be up to 6 m thick.

Keywords: Geographe Bay, Sandbars, Palaeochannels, Low-relief ridges, Sea level oscillations

Manuscript received 6 December 2018; accepted 27 August 2019

INTRODUCTION

Geographe Bay, between Cape Naturaliste and the city of Bunbury, in the south-western corner of Western Australia, lacks major fluvial sediment input and is considered sediment starved like much of the state's coastline (McMahon & Finlayson 2003; Brooke *et al*. 2017). Consequently, much of the sediment available for shoreline nourishment is sourced by the remobilisation of relict siliciclastic sediments deposited on the inner shelf during sea-level lowstands, and from carbonate organisms (such as coralline algae, molluscs, foraminifera and bryozoans), which are produced in and around the extensive seagrass banks that characterise Geographe Bay (James & Bones 2010; Brooke *et al*. 2014). The relict siliciclastic grains within the inner shelf are a finite resource as the volume of sediment available for transport onshore is limited by wave energy, water depth and grain size (Whitehouse 2007). In contrast, carbonate grains are continually being produced and can potentially provide a sediment resource for coastal nourishment. However, the supply of carbonate sediment to the coast is limited by the rates of carbonate production, which can be influenced by changing environmental parameters such as sea-surface temperature, nutrient availability and habitat change (James & Bone 2010), as well as hydrodynamic processes.

The Geographe Bay coastline is fringed by a series of low-relief coastal eolianites and dunes (Brooke *et al*. 2014), with sections of the coast presently experiencing coastal erosion, the cause of which is still poorly understood (Geographe Catchment Council 2008; Barr & Eliot 2011, Barr *et al*. 2017). Thus there is a need to better characterise the marine-sediment resources, particularly in a context of shoreline behaviour within a sediment-starved coastal environment, under rising sea levels and changing wave climate.

The aim of this study was to better understand local coastal evolution, the sediment resource potential of Geographe Bay, and the influence that geomorphology, hydrodynamics and habitat have on sediment mobility and onshore transport. An integrated approach was adopted, combining high-resolution bathymetry, sedimentological analysis, hydrodynamic data and high-resolution reflection-seismic images, conducted between Busselton and Port Geographe (Geographe Bay, Rottnest Shelf, south-west Western Australia).

The lithology and age of inner shelf deposits were inferred from previous investigations from Geographe Bay to Rottnest Island (including the Swan Coastal Plain; e.g., Probert 1967; Playford *et al*. 1976; Wharton 1981, 1982; Commander 1982; Hirschberg 1988, 1989; Deeney 1989; Collins and Baxter 1984; Hamilton & Collins 1997; Schafer *et al*. 2008; Brooke *et al*. 2010, 2014) because coring and dating was not part of the present study. Interpretation of the geomorphological features is supported by the findings of Brooke *et al*. (2010, 2014) who carried out an extensive morphostratigraphic investigation of shore-parallel, relict barriers and ridges between Hillarys (30 km north of Rottnest Island) and Cockburn Sound (up to 34 km south of Rottnest Island), using bathymetric and topographic digital relief models and previously acquired dating (from Price *et al*. 2001 and Hearty 2003). Several shallow cores (up to 6 m long) cut within Cockburn Sound (about 100 km north of the survey area) by Skene *et al*. (2005) provide valuable insights into the sub-seafloor deposits of south-west Australia and were used to support the interpretation of the shallow stratigraphy proposed in this study. Of fundamental importance for the inferred chronostratigraphy of the survey area, are the geotechnical, sedimentological and palynological data obtained through the 'Quindalup borehole line project' (Wharton 1981, 1982) and the 'Busselton shallow-drilling project', (Hirschberg 1988, 1989) on the Swan Coastal Plain between Dunsborough and Capel (Fig. 1), as part of an assessment of the groundwater resources of the Perth Basin. Although the majority of these studies were investigating groundwater aquifers, the findings derived by collecting terrestrial borehole sediment can be extended to the nearshore marine area, due to proximity of the boreholes to the coastline.

REGIONAL SETTING

Coastal physiography

Geographe Bay is a 90 km long, J-shaped bay with a west-northwest aspect in the north and north-west through to north-east in the south (Fig. 1). The nearshore bathymetry is relatively simple with a shallow-dipping seabed reaching 30 m depth about 15 km from the coast. However, the south-westernmost section between Dunsborough and Cape Naturaliste is characterised by a steeper bathymetric gradient with water depths reaching 40 m within 1 km of the coast (Fig. 1).

The region is characterised by a Mediterranean climate, warm and dry between November and March (summer) and cool and wet in winter (Bureau of Meteorology - Australia 2011). There is only one permanent river (Capel River; Fig. 1, no. 16) that discharges directly into the ocean (mean annual flow of 39.9 Gigalitres (Department of Water 2008), the other waterways are ephemeral or seasonal and flow

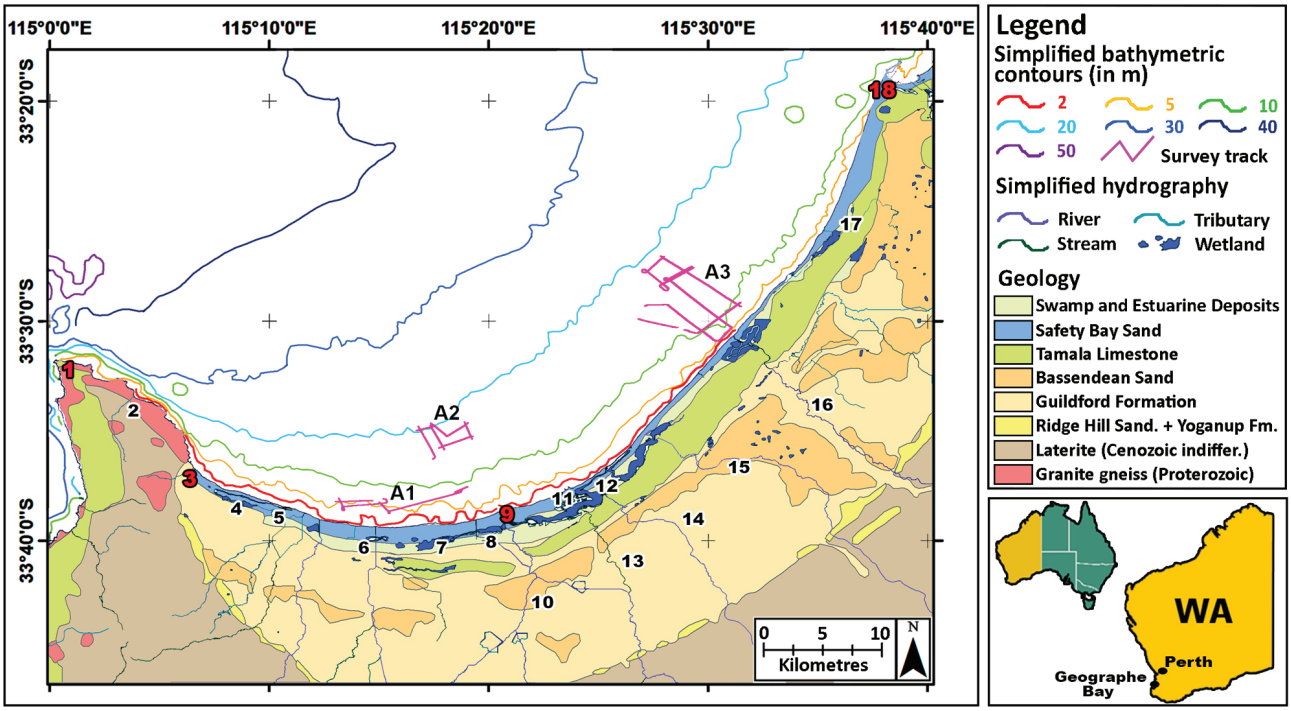

Figure 1. Geographe Bay map showing simplified surface geology (redrawn after Playford *et al*. 1976), localities (red labels) and bodies of water (black labels). 1 Cape Naturaliste, 2 Jingarmup Creek, 3 Dunsborough, 4 Toby Inlet, 5 Toby drain, 6 Quindalup, 7 Broadwater–New River, 8 Vasse-Diversion drain, 9 Busselton and Busselton Jetty, 10 Vasse River, 11 Port Geographe Marina, 12 Vasse–Wonnerup Estuary, 13 Sabina River, 14 Abba River, 15 Lundlow River, 16 Capel River, 17 Mile Brook diversion, 18 Point Casuarina (Bunbury). A1, A2 and A3 are the seismic survey locations. The geophysical survey track plot is also marked (in pink). Hydrography: Linear (Hierarchy; Department of Water DOW-029; 29-10-2008 12:18:04) from Shared Location Information Platform (SLIP; WMS Server: https://www2.landgate.wa.gov.au/ows/wmspublic?; Service Name: SLIP Public Web Map Service (ISO 19115 Categories). Simplified bathymetric contours are shown (source: Department of Transport).

mainly into drains (White & Comer 1999). Extensive seagrass meadows (*Posidonia sinuosa* and *Amphibolis antarctica*) represent the major benthic habitat within the bay, covering more than 90% of the seabed down to 10 m below sea level (Van Niel *et al*. 2009). The seagrass coverage decreases progressively northward and with depth, down to 30 m below mean sea level (BSL; Oldham *et al*. 2010).

Geographe Bay, like in the rest of south-western Australia, experiences a diurnal microtidal regime with a spring tidal amplitude on the order of 0.6 m (CSIRO 2015). Winds are mainly seasonal: the summer period is dominated by relatively light to moderate south to south-westerly offshore sea breezes (up to 15 m/s, in the afternoon) while strong south-westerly to north-westerly winds (up to 25–30 m/s), associated with cold fronts, occur periodically during the winter months (Fahrner & Pattiaratchi 1994; Oldham *et al*. 2010). The wave regime is mostly dominated by the seasonal winds, with waves typically reaching heights of up to 2 m in winter and less than 1 m in summer (Fahrner & Pattiaratchi 1994; Oldham *et al*. 2010). Surface waves are also influenced by an oceanic southwest swell, with Cape Naturaliste refracting waves into Geographe Bay, protecting the coast from the prevailing long-period ground swell (Fahrner & Pattiaratchi 1994; Oldham *et al*. 2010).

Coastal currents and water-circulation patterns are mainly wind driven, including storm waves, sea breezes and local bathymetry (Fahrner & Pattiaratchi 1994; Oldham *et al*. 2010). These metocean processes generate eastward to north-eastward longshore currents that influence sediment transport, control the seafloor sediment characteristics and are ultimately reflected in the sedimentary record (Paul & Searle 1978; Hamilton & Collins 1997; Oldham *et al*. 2010). Seagrass meadows also have a significant role in the overall hydrodynamic conditions of the bay, attenuating wave and current energy and sediment particle transport (McMahon *et al*. 1997; Oldham *et al*. 2010).

Coastal Geology and Geomorphology

Geographe Bay lies on the south-western Australian continental shelf margin (Fairbridge 1961; Baker *et al*. 2005) within the southern Perth Basin—a Phanerozoic, intensely faulted half-graben, infilled with about 15 km of Paleozoic – Lower Cretaceous clastic strata and Lower Cretaceous – Holocene carbonate sediment (Collins & Baxter 1984). The area has been relatively tectonically stable since the Mid-Pleistocene (Playford *et al*. 1976, Szabo 1979; Kendrick *et al*. 1991; Stirling *et al*. 1995; Baker *et al*. 2005; Brooke *et al*. 2014).

The Lower Cretaceous Leederville Formation, which consists of fine- to medium-grained quartz sandstone interbedded with shale, is inferred to be mostly non-marine, with minor shallow-water near-shore marine horizons (Playford *et al*. 1976; Deeney 1989; Hirschberg 1989; Schafer *et al*. 2008). The formation is unconformably overlain by Quaternary superficial units, predominantly sand and limestone in the west, and lacustrine clay in the east (Deeney 1989; Hirschberg 1989). The superficial deposits, collectively known as the Kwinana Group, form the Swan Coastal Plain, a narrow strip (10–15 km wide) of reworked Quaternary sediment that comprises shallow marine and littoral deposits, and associated fossil eolian dunes aligned sub-parallel to the coastline (Collins 1988; Commander 2003). Fluvial, alluvial and lacustrine deposits are also present (Playford *et al*. 1976; Hirschberg 1989). The shoreline successions become progressively younger and decrease in elevation westward. These comprises the Ridge Hill Shelf (possibly Lower Pleistocene Ridge Hill Sandstone); Yoganup Shoreline deposits (possibly Middle Pleistocene Yoganup Formation), the Bassendean, Spearwood and Quindalup Dune Systems, respectively the Middle–Upper Pleistocene Bassendean Sand, eolian limestone and yellow sand of Tamala Limestone; and Holocene marine and eolian parabolic dunes and the Safety Bay Sand (Playford *et al*. 1976; Commander 2003; Fig. 1).

The Rottnest Shelf, defined by Carrigy & Fairbridge (1954), can be subdivided into three main bathymetric provinces: (1) the Inner Shelf, which extends from 0 to 100 m in depth, where submerged terraces and ridges formed during past periods of low sea level (Fig. 1); (2) the Outer Shelf that ends with the shelf–slope break at 170 m; and (3) the Upper Continental Slope (Collins 1988). Traces of subaerial erosion are recognisable in remnant subaqueous features such as reefs, shore-parallel ridges and barrier-dune systems (Collins 1988; Playford 1997; Brooke *et al*. 2010).

METHODS

Seafloor mapping

In 2016, the Western Australian Department of Transport (DoT) acquired and processed bathymetric datasets, during multiple LiDAR (Light Detection and Ranging), multibeam and Laser surveys (Coastal Information, DoT 2016). The high-resolution data have a horizontal sounding density of 5 x 5 m and cover the nearshore seafloor up to about 30 m water depth (Coastal Information, DoT 2016).

A map of the main seafloor features was produced through a visual interpretation of the bathymetry, using ESRI's ArcGIS Desktop 10.5. The surficial geomorphological features were manually outlined at a 1:10 000 scale and include sandbars, palaeochannels and ridges.

The morphological information was used to determine which areas within the bay to carry out the following seismic survey. Three distinct areas (A1–3; Fig. 1) were selected for detailed seismic investigation and sediment sampling: (1) A1 in the westernmost portion of the investigation area is characterised by a high concentration of sandbars, oblique to the shoreline; (2) A2, 6 km seaward from Busselton Jetty, has numerous deep-water (~20 m) ridges and palaeochannels; and (3) A3, in front of the Capel River mouth, is distinguished by several shallow-water (<10 m) ridges and palaeochannels.

High-resolution shallow-seismic data acquisition

A total of 71 km of high-resolution reflection seismic profiles were acquired between the mouths of Buayanup drain and Capel River (A1, A2 and A3, Fig. 1). The main track orientations were parallel and perpendicular to the coastline, to capture most elements of the seafloor

morphology. In A1, the seismic survey covered 16 km, mainly oriented north-northeasterly to south-southwesterly, in water depths of 5–10 m. A total of 15 km of seismic profiles were collected within A2, in relatively deep waters (~15–22 m). A3 comprises 40 km of seismic tracks, mostly orthogonal to the coastline, between ~8 and 22 m water depth.

The seismic survey was undertaken using an Applied Acoustic Boomer System, comprising an energy source (CSP-P 300) and a sound source (AA201 boomer plate), mounted on a surface-tow catamaran. An 8-element hydrophone streamer was employed as receiver. A GNSS (Global Navigation Satellite System) receiver Trimble NetR9 was interfaced to the acquisition workstation, broadcasting NMEA string to the geophysical software (SonarWiz 6 V6.01.0024, Chesapeake Technology Inc.). Data was digitally recorded in Seg-Y format and real-time quality control was done during data collection.

SonarWiz 6 software was also employed for data processing. The first step of post processing was bottom tracking, which is used to digitise the seafloor reflector. In the second step, standard signal processing procedures, such as application of Time Varying Gain (TVG) and enhancing the contrast, were applied to improve the signal to noise ratio. In the final step, sub-bottom horizons were digitised with manual picking. Based on the local geology and the speed of sound in sediments (see Whiteley & Stewart 2008; Duncan *et al*. 2009; Duncan & Gavrilov 2012), the depth below the seafloor and the sediment thickness values were depth converted using an estimated propagation velocity of 2000 m/s. Given a margin of error of about ±50 m/s, the vertical error is ~0.5 m.

Sediment sampling and analysis

A pipe dredge was used to collect 17 unconsolidated surficial sediment samples along areas A1 (10 samples) and A2 (7 samples). Sampling location coordinates were recorded directly into SonarWiz 6, using the same positioning system used for the seismic survey.

The samples were dried and sieved using a mechanical shaker, over 63 µm, 125 µm, 250 µm, 500 µm, 1 mm and 2 mm meshes, and examined using a stereoscopic light microscope. Analysis of the sediment included an evaluation of colour using the Munsell Soil Chart (Munsell 1954), estimation of shape (roundness/sphericity of individual grains) and identification of the mineral and biogenic components.

RESULTS

Shallow stratigraphy

The shallow seismic survey allowed the characterisation of the internal architecture of the sub-surface reflectors and identification of stratigraphic features, down to a depth of approximately 30–40 m below the seafloor. The sub-surface reflectors TB (top Unit B) and TP (top Unit P) bound three discrete seismic units (from bottom to top: B, P and H, respectively; Fig. 2). Two minor reflectors (TP1 and TP2) also have been detected within Unit P along the survey area.

UNIT B

TB (green in the seismic interpretation; Fig. 2) is the deepest reflector recognised in the study area, ranging between ~15 m and 30 m below sea floor (~27 m BSL in A2 and ~47 m BSL in A3). Where detected, TB appears to be mostly relatively flat and laterally continuous. In A2 and A3, where profiles orthogonal to the coastline are longer (2.5–6 km), TB is clearly seen deepening offshore, lying sub-parallel to the modern seafloor. In several coastal-parallel profiles, irregular incisions can occasionally be recognised.. The TB reflector caps a low amplitude and seismically chaotic unit (Unit B), No other main seismic reflectors can be recognised below TB, for this reason, TB can be considered the top boundary of the acoustic basement.

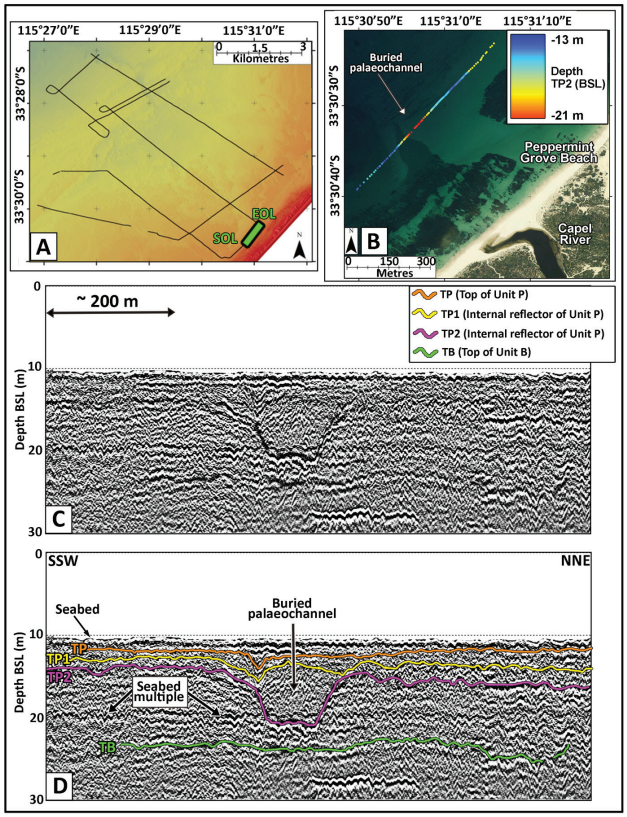

Figure 2. Example of seismic profile, showing the two main seismic reflectors depicted in the survey area (TP and TB) and two secondary reflectors (TP1 and TP2). A: Seismic tracks for Area 3. The location of the profile reported in C, D is highlighted in green (SOL: start of line, EOL: end of line). B: Orthophoto from SLIP (Shared Land Information Platform; Enabler portal, Landgate Imagery Bunbury 2031 Oct–Nov 2010 Mosaic). The buried palaeochannel is clearly visible when plotting the depth of the reflector TP2 (from sea level). C, D: uninterpreted and interpreted seismic profile. Note the well-defined buried palaeochannel. The vertical axis corresponds to the depth below sea level (BSL) and the scale is in metres. The sound velocity in the sediments is equivalent to ~2000 m/s. The horizontal axis represents the distance covered by the vessel and the scale is in metres.

UNIT P

Reflector TP (shown in orange, Fig. 2) is well resolved in area A1 and in the profiles close to shore in A3. This sharp reflector is undulated to irregular, with several depressions and incisions and marks the top of Unit P, which is bounded between TP and TB. The internal reflection character of Unit P varies across the survey area and ranges from chaotic or reflection-free, to poorly or moderately stratified. Two minor reflectors can occasionally be recognised within this unit (TP1 and TP2). TP1 is mostly recognisable near shore, especially in A3 (depicted in yellow in the seismic interpretation, Fig. 2). This secondary reflector is generally flat, with some channel-like depressions, up to 250 m wide and 11 m deep. TP2 is normally present in A2 and A3 (2) and, as with TP1, it appears relatively flat, with intermittent depressions up to 7 m deep (Fig. 2C).

UNIT H

Unit H is bounded between the seafloor and the reflector TP. Where TP is detected, the thickness of this surficial unit ranges from less than 50 cm to about 6 m and averages 1–3 m. In some areas, a strong return signal of the seafloor, seabed multiples and local poor imaging mask this unit (and consequently the ability to detect the underlying horizons TP and TB). In addition, it is likely that in some places, especially in the offshore profiles, Unit H is too thin to be detected with the equipment used (vertical resolution of the boomer is approximately 30 cm) or is absent; these uncertainties made the interpretation of Unit H potentially ambiguous. Some parallel stratified reflections can be identified within Unit H.

Seabed features

High-resolution bathymetry highlights three main geomorphic features that characterise the seabed morphology in Geographe Bay, these are sandbars, palaeochannels and ridges (Fig. 3).

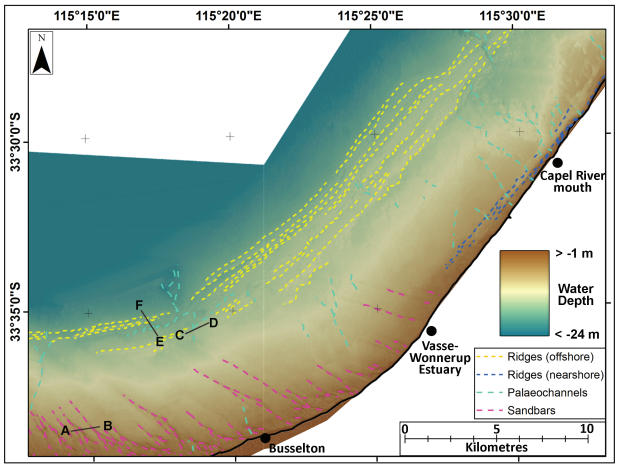

Figure 3. Composite bathymetric data (from Department of Transport) overlaid by seabed features. White areas: no data. Profile A–B: see Figure 4. Profile C–D: see Figure 5. Profile E–F: see Figure 6.

SANDBARS

The sandbars and associated swales are near-continuous linear features that extend obliquely (at an acute angle to the shoreline of 15–30°) from nearshore, up to ~6 km seaward (between Geographe and West Busselton), to a water depth of 10 m. They mainly lie in the south-western portion of the bay, with the easternmost sandbar lying in front of the northern tip of Vasse–Wonnerup Estuary (location 12 in Figs 1, 3). The distance between successive sandbar crests increases to the north-east, ranging from about 250 m to more than 1.5 km. These sandbars vary greatly in size from about 100–300 m wide with the dune crest up to ~3 m above the seabed, and thin seaward. They are generally asymmetrical, with an almost bare stoss flank and a vegetated lee side (Fig. 4).

PALAEOCHANNELS

The high-resolution bathymetric and seismic images revealed the presence of several partially buried and surficial palaeochannels, assembled predominantly around Area 1 and Area 3, respectively (see surficial palaeochannels marked in light blue in Figs 3, 5).

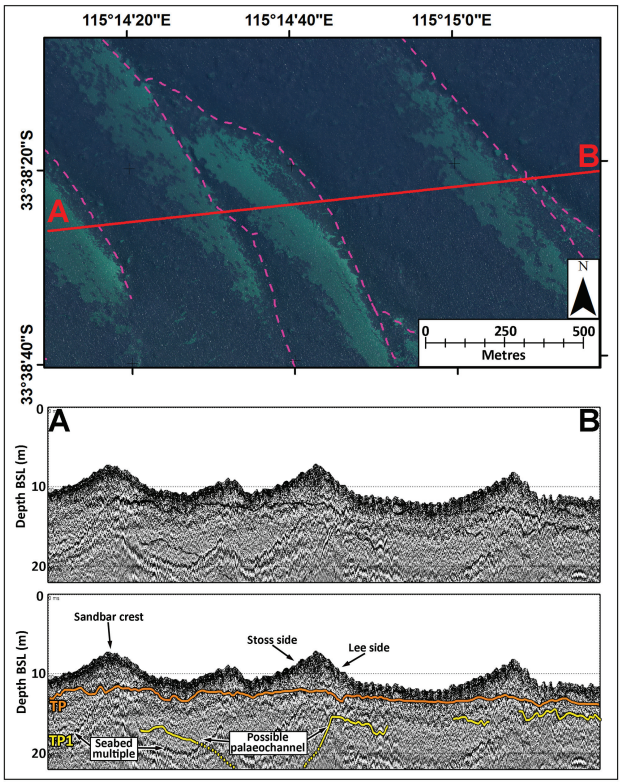

Figure 4. Profile A–B: sandbars, for location refer to Figure 3. Length: ~1755 m. Top: orthophoto from SLIP Enabler portal (Landgate Imagery). Darker colours represent areas covered with seagrass meadows. Pink dash line depicts the crest of the sandbars. Bottom: uninterpreted and interpreted seismic profile showing the buried architecture below the sandbars. The reflector TP is almost flat; conversely, reflector TP1 is irregular with a possible palaeochannel, marked with dash line. The vertical axis corresponds to the depth below sea level (BSL) and the scale is in metres. The sound velocity in the sediments is equivalent to ~2000 m/s.

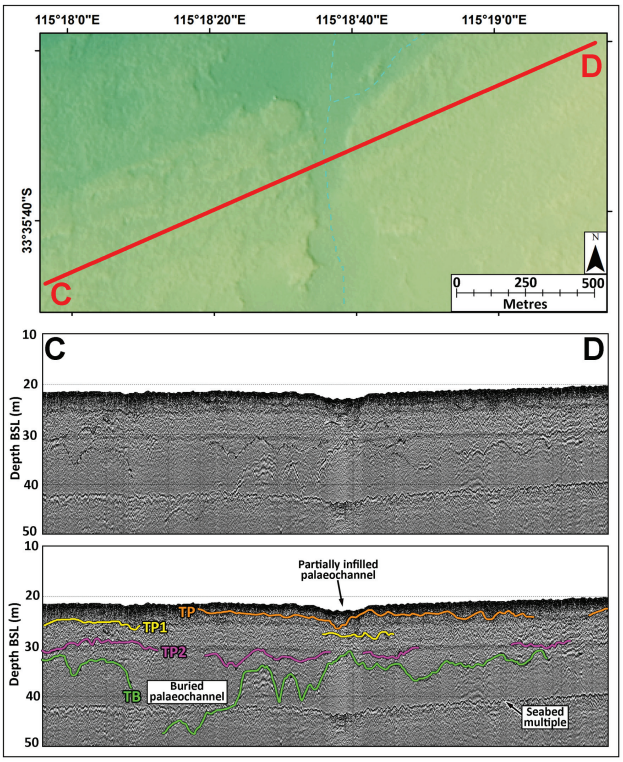

Figure 5. Profile C–D: palaeochannels, for location refer to Figure 3. Length: ~2175 m. Top: composite bathymetric data (from DoT) through the offshore channel. The light blue dash line depicts the thalweg of the surficial channel. Bottom: uninterpreted and interpreted seismic profile revealing a deeper buried palaeochannel. The palaeochannel is almost entirely infilled with sediment belonging to Unit H. The vertical axis corresponds to the depth below sea level (BSL) and the scale is in metres. The sound velocity in the sediments is equivalent to ~2000 m/s.

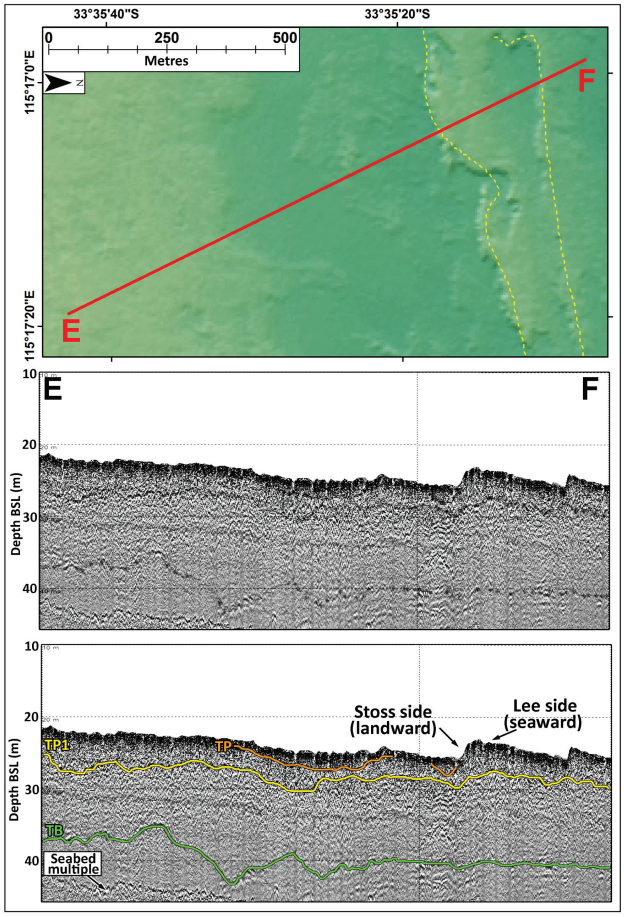

Figure 6. Profile E–F: ridges, for location refer to Figure 3. Length: 1215 m. Top: composite bathymetric data (from DoT). Yellow dash line depicts the crest of the ridges. Note: the layout of the map has been rotated by 270° to match the orientation of the seismic profile. The north arrow has been adjusted accordingly. Bottom: uninterpreted and interpreted seismic profile displaying the sub-surficial architecture; note Units P and H are not clearly discernible. The vertical axis corresponds to the depth below sea level (BSL) and the scale is in metres. The sound velocity in the sediments is equivalent to ~2000 m/s.

The surficial features have a variable length, from a few hundred metres to ~6 km, and are generally perpendicular to the coastline and quite shallow, with an average depth ~1 m below the surrounding seabed.

LOW-RELIEF RIDGES

Further significant geomorphic features that characterise the seabed in Geographe Bay are the linear, shore-parallel, low-relief ridges (Fig. 6).

Two distinct groups are observed: (1) the deep-water ridges that lie 6–9.5 km from the shoreline at depths of ~15–20 m; and (2) the shallow-water ridges, which are found only in the north-eastern portion of the bay and are within 1 km from the coast in water depths <7 m (Fig. 3). Cross-section transects indicate that the ridges have an uneven profile, with an almost flat top, a steep stoss end landward and a gentle lee slope seaward (Fig. 6), with a relief of less than 3 m. The deep-water ridge crests are sub-parallel and between 200 and 900 m apart, whereas the shallow-water ridges are more closely spaced, and their crests are between 100 and 500 m apart.

Sediment distribution

In A1, the samples collected along the sandbars range mainly from coarse sand (0.5–1 mm, in green) to medium sand (0.25–0.5 mm; purple fraction in Fig. 7). Very coarse material (>2 mm) is entirely made up of biogenic skeletal grains that are highly variable in size (up to 3.5 cm in diameter) and consists mostly of fragmented or whole gastropods, but also includes bivalves, foraminifera and scaphopods. Overall, the sediment is pale yellow (Munsell colour, 10YR, 8/3 to 7/4). The mineral composition is mixed carbonate–silicate sand, dominated by quartz, which reaches ~60% of each bulk sample. In the finer fraction, quartz is dominant, representing about 85–90% of the sediment having grain dimensions <1 mm. The quartz grains generally display a medium to low sphericity and are predominantly sub-angular to rounded. They are mainly clear, translucent

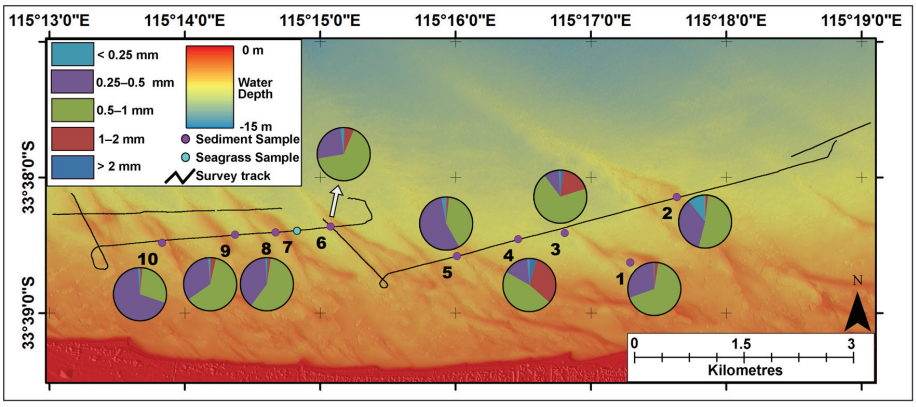

Figure 7. Surficial sediment distribution superimposed on composite bathymetric data (from DoT). Each pie chart illustrates different grain size distribution in the sediment collected in Area 1. Sediment typically ranges from medium sands (0.25–0.5 mm, in purple) and coarse sands (0.5–1 mm, in green). Note: sample 7 contained only seagrass debris.

to frosted, generally with crescentic impact marks, but occasionally, they appear frosted and yellow, orange to light brown. The remaining sediment comprises bioclasts (especially in samples 3, 4 and 6), minor feldspar, rock fragments, possible red/brown garnet and black heavy minerals, particularly in finer grains. Finer siliciclastic sediments (medium to fine sand) are more dominant on sandbar crests. Coarse and very coarse material, generally bioclastic in origin, tends to accumulate in the troughs between sandbars, such as in samples 3, 4 and 6 (Fig. 7).

In A2, the sediment sampled from the top of the deep-water ridges is coarser and contains a larger amount of quartz than along the sandbars (Fig. 8) in which finer particles are also present. The quartz grains are colourless, yellow or red to brown, generally translucent to transparent, sub- to well-rounded, with variable sphericity. The biogenic fragments include broken mollusc shells, foraminifera and coralline algae. Bryozoans and larger lithified fragments are also present; the latter consist of a mixture of detrital quartz and sand-sized biogenic fragments, with carbonate cement (calcite), indicating the calcarenite origin of the hard surface close to the seafloor. The biggest piece of this calcarenite (10 x 6 x 1.5 cm) was collected in sample 14.

Grain size of sediment around the deep-water ridges decreases seaward, where the medium-sand content increases (for instance, sample 11, Fig. 8). The availability of unconsolidated sediment also diminishes farther offshore. At some sites, several attempts at sediment sampling were unsuccessful, due to the indurated nature of the seafloor. As on the sandbars, coarser material is found in depressions (samples 12, 15, 16 and 17) and finer material on crests (i.e. sample 14).

STRATIGRAPHIC INTERPRETATION

In several places, no reflectors could be identified beyond the seafloor due to a combination of factors that significantly reduced the quality of the seismic imaging. Hard bottoms and lack of velocity contrast between the buried lithologies are inferred to be the main causes of signal attenuation and limited acoustic penetration. In addition, dense seagrass is likely to have affected

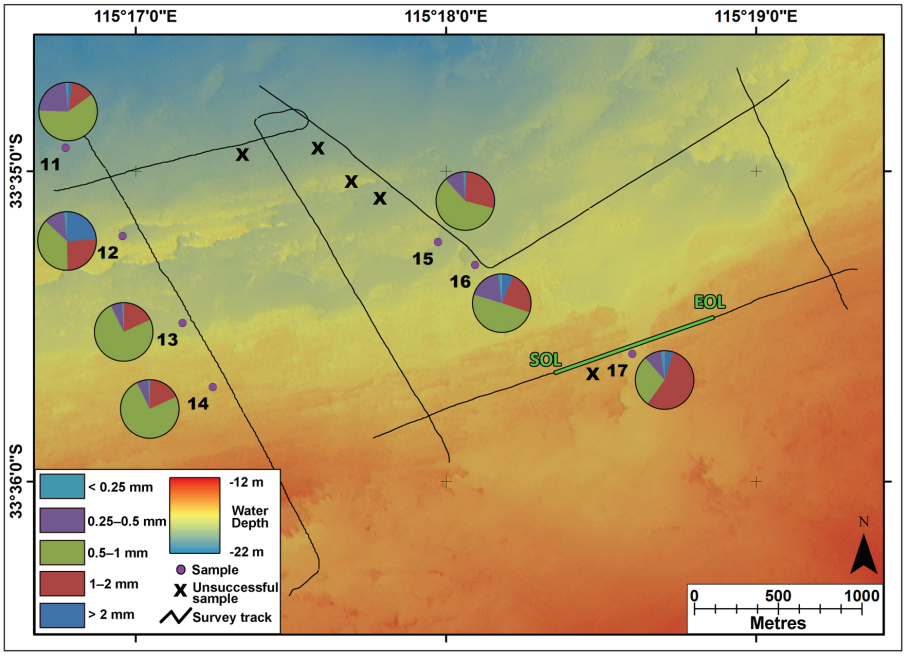

Figure 8. Surficial sediment distribution superimposed on composite bathymetric data (from DoT). As in Figure 7, each pie chart illustrates different grain size distribution in the sediment. In Area 2, sediment ranges mainly from coarse sands (0.5–1 mm, in green) and very coarse sands (1–2 mm, in red). The black cross symbols represent stations where sampling was unsuccessful due to the hard substrate. The green line marks the location of the seismic profile in Figure 12. SOL: Start of Line; EOL: End of Line.

the propagation of the signal, causing scattering and consequent deterioration of the quality in the acquired profiles. Acoustic multiples and ringing also were additional issues in some profiles as the reflections mask the deep reflectors (refer to Kearey *et al*. 2002).

The following chronostratigraphic interpretation is based on the findings of previous investigations carried out by the Geological Survey of Western Australia (Wharton 1981, 1982; Hirschberg 1988, 1989; Deeney 1989). During these studies, which aimed to define the lateral and vertical extent of the local aquifer systems, three clusters of boreholes were drilled near the shoreline adjacent to Area 1 (just west of Busselton, Figs 1, 9). The bore completion reports (Hirschberg 1988) showed that the shallow stratigraphy, up to 50 m below the Australian Height Datum (AHD) includes three successive units): (1) the Lower Cretaceous Leederville Formation (Unit B, basement); (2) the Pleistocene Tamala Limestone (up to 15 m thick); and (3) Holocene deposits (maximum thickness of 10 m; Fig. 9).

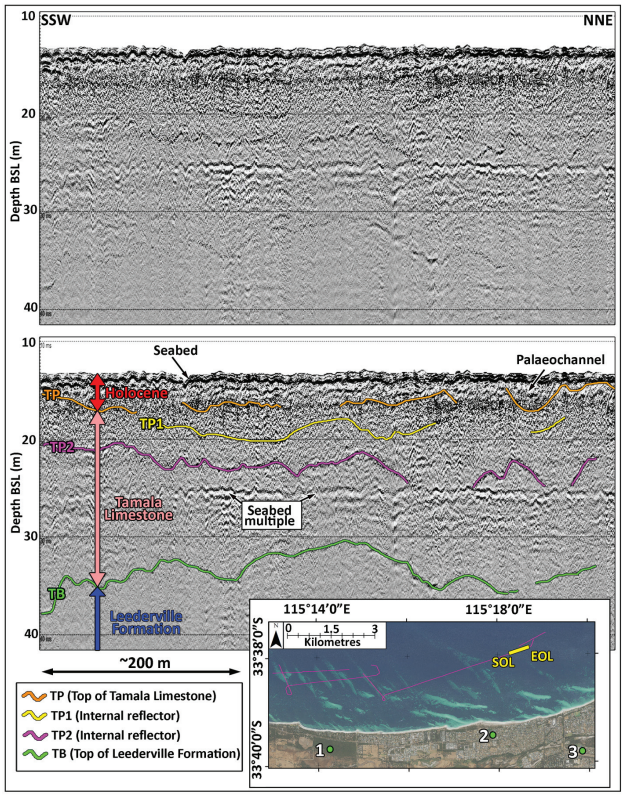

Figure 9. Top: uninterpreted seismic profile. Bottom: interpreted seismic profile. The vertical axis corresponds to the depth below sea level (BSL) and the scale is in metres. The sound velocity in the sediment is equivalent to 2000 m/s. The horizontal axis represents the distance covered by the vessel and the scale is in metres; in the insert location of the line, recorded in Area 1. The dots represent the boreholes collected by Wharton (1981, 1982) and Hirschberg (1989). Orthophoto section from SLIP (Shared Land Information Platform) Enabler portal, Landgate Imagery (Busselton Shire Jan 2016 Mosaic).

Unit B: Leederville Formation

Based on the sedimentological records, the newly acquired seismic data and the available literature (e.g. Probert 1967; Wharton 1981, 1982; Deeney 1989; Hirschberg 1989; Collins & Baxter 1984; Hamilton & Collins 1997), the intensely scoured Unit B is interpreted as the Leederville Formation, a Lower Cretaceous succession of interbedded sandstone with siltstone and claystone (Cockbain & Playford 1973; Playford *et al*. 1976). Wharton (1982) and Hirschberg (1989) described the formation as weakly consolidated, fine- to coarse-grained sandstone interbedded with silty dark carbonaceous shales (Fig, 9). Accessory minerals, including heavy minerals, feldspar and pyrite, are common (Wharton 1981, 1982; Hirschberg 1989). It is likely that the heavy minerals found in the surficial sediments, collected in Area 1 and Area 2, are derived from erosion of the Leederville Formation, during the Plio-Pleistocene, when several cycles of sea-level variation controlled the deposition and reworking of these minerals, especially along the shoreline (Collins & Baxter 1984). The borehole logs also show that the Leederville Formation is unconformably overlain by the Pleistocene Tamala Limestone (Wharton 1981, 1982; Hirschberg 1989).

Unit P: Tamala Limestone

Based on the findings of Wharton (1981, 1982) and Hirschberg (1989), it is possible to assume that Unit P corresponds to the Tamala Limestone. These authors described the formation as light-brown to orange, fine to coarse, bioclastic sand and limestone. Several other studies that have investigated the sub-surficial geology of Geographe Bay and adjacent areas, support the proposed interpretation of Unit P, including Paul & Searle (1978), Collins (1988) and Skene *et al*. (2005). The latter carried out an extensive coring program in Cockburn Sound and intersected the top of Tamala Limestone in several cores.

The Tamala Limestone forms a coastal strip, roughly parallel to the present shoreline, extending up to 10 km inland and 30 km offshore (inner shelf, Brooke *et al*. 2010) and stretches along the state's coast for more than 1000 km, from the South West to Shark Bay in the north (Fig. 1, right bottom corner). The formation represents a series of shoreline deposits and associated eolianite build-ups (cemented dunes), composed of coastal carbonate sediment and quartzose sand (Brooke *et al*. 2010), deposited during Pleistocene marine transgressive events (Brooke *et al*. 2014).

Since the Tamala Limestone is strongly diachronous, with a deposition spanning the Mid–Late Pleistocene to Early Holocene (Murray-Wallace & Kimber 1989; Brooke *et al*. 2014; Gozzard 2007), the minor reflectors within Unit P (TP1 and TP2) likely represent different periods of deposition, diagenesis and erosion of the formation, and reflect different stages of sea level. Palaeochannels are the confirmation of these oscillations. Palaeochannels that were incised during lowering sea level and successively infilled by more recent sediment are common within Unit P (Fig. 2).

Unit H: Holocene unit

It can be assumed that the sediments belonging to Unit H are a thin blanket of Holocene deposits, over the Tamala

Limestone. Several authors have investigated the marine Holocene deposits along the Western Australian coast, in order to understand the timing of marine inundations. For instance, Baker *et al*. (2005) dated relict formations of inter-tidal serpulid tubeworms (vertical resolution as sea-level indicators: ±25 cm, following Baker & Haworth 1997; Baker & Haworth 2000 and Baker *et al*. 2001) from 21 locations along southern Western Australia, from Rottnest Island to Esperance (Fig. 1). Their research demonstrated that sea level peaked about 2.0 m above present between 6600 and 6800 years Before Present (BP), followed by an uneven fall to the present. Notably, a similar timing and elevation of the peak Holocene sea level was identified by Jahnert & Collins (2013) and Bufarale & Collins (2015) in Shark Bay. According to the composite Holocene sea-level curve for the Houtman Abrolhos Islands (Collins *et al*. 2006), it is likely that the sea inundated the inner shelf in Geographe Bay during the early Holocene, around 10 thousand years (ky) ago, when the base (sea) level reached the modern isobath of 20 m.

From the sediment analysis, the deposits are a mixture of relict siliciclastic grains, with a variable component of bioclasts. The thin ferruginous coating on the siliciclastic grains in Area 2 suggests that the sediment is reworked material of the Cooloongup Sand, a unit derived from the residual deposits left from Tamala Limestone dissolution (Lipar & Webb 2014). The light yellow to cream quartzose sediments in Area 1 may have originated from the reworking of the Burragenup Member, a Holocene unit of the Safety Bay Sand, composed of remnants of cemented dunes (Lipar & Webb 2014). In contrast, the carbonate grains are more recent and linked with the development of \seagrass meadows.

Unit H cannot be clearly recognised in deeper water (in A2 and part of A3, between 15 and 20 m BSL), using a seismic device. This is an important observation suggesting a very limited Holocene cover. In an essentially sediment-starved environment like Geographe Bay, where the riverine input of siliciclastic sediment is limited, it is possible to credit the importance of seagrass as a key-feature in sediment production and deposition. Seagrasses in fact not only produce *in situ* biogenic deposits, but also represent significant trapping and binding agents of the unconsolidated sediment (Hendriks *et al*. 2008; Gibbes *et al*. 2014; Bufarale & Collins 2015). This remark is in apparent contrast with the results of the sediment analysis, which show quartz as the dominant component. In this area, it is likely that hydrodynamic sorting also affects the lithological distribution. Bioclasts and quartz have in fact, significant hydrodynamic differences: carbonates are less dense, platy and have a greater surface area, therefore are easily subject to hydrodynamic sorting, whereas quartz grains are denser and less prone to be transported (Longhitano 2011; Chiarella *et al*. 2012). As a result, the carbonate sediment is reworked and transported onshore by waves (Brooke *et al*. 2014), and siliciclastic grains remain trapped within the sandbars, which act as a sediment sink, on the inner continental shelf.

GEOMORPHOLOGICAL FEATURES

The end of the Marine Isotope Stage 5e (MIS) climatic optimum (~118 ky BP) was characterised by a rapid marine regression, coinciding with an insolation minimum and cooler global temperatures (Lambeck & Chappell 2001; Lambeck *et al*. 2002; Bianchi & Gersonde 2002; Hearty *et al*. 2007). For the following ~110–7 ky BP, the sea level was lower than at present (Collins *et al*. 2006; Jahnert & Collins 2013; Bufarale *et al*. 2017). During this time, the Capel River and other river systems in the region deposited siliciclastic sediment on the shelf, and waves and currents mobilised terrigenous grains longshore, trapping some in Geographe Bay (Collins 1988). Coarser grains are mostly confined to palaeochannels or topographic lows whereas finer sediments were deposited on the palaeo-shoreface and then transported along the coast. During the late Pleistocene – early Holocene sea-level oscillations siliciclastic material was intensively reworked (and rounded) and transported seaward by fluvial and eolian processes under falling sea level and landward by waves and currents under rising sea level (Collins 1988).

Around 10 ky BP, a marine transgression led to significant changes to sediment erosion, transport and deposition in Geographe Bay. The inner shelf became submerged and waves and currents started to mobilise the unconsolidated siliciclastic grains, forming longitudinal sandbars, which are presently aligned with

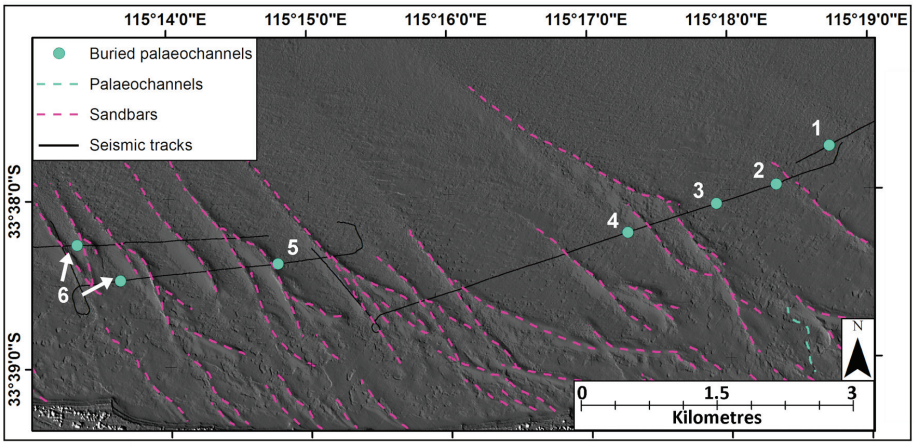

Figure 10. Location of sandbars (pink dashed line) and buried palaeochannels (identified with the seismic profiles, marked in light blue dots) in area A1. Surficial palaeochannel incisions are also delineated (light blue dashed line).

prevailing wave direction and partially covered with seagrass. In contrast to the ridges, these features are likely to have a quartz-dominated core, with a veneer of carbonate material (Paul & Saerle 1978). Although the sediment directly beneath the seagrasses was not sampled, samples from the exposed stoss side showed that the bar is quartz-dominated, supporting this interpretation.

Sandbars

In Geographe Bay, the oblique sandbars, first described by Paul & Searle (1978), are all subparallel (Fig. 10). Superimposing the sandbar map distribution (from Fig. 10) to the mean wave direction chart (Fig. 11), the interaction between these elements is highlighted, with the sandbars positioned perpendicular to the mean wave direction. The mean wave direction chart shows how the south-westerly storm waves are refracted around Cape Naturaliste toward Geographe Bay coast (Pattiaratchi & Wijeratne 2011), clearly playing a significant role in mobilising the sediment and creating the sandbars. These observations have been investigated by Pattiaratchi *et al*. (2011, 2015, 2017) who reviewed the impact that the construction of Port Geographe had on the local shoreline evolution. Using a computer program simulating waves, water flow and sediment transport, coupled with bathymetric and LiDAR data, these researchers confirmed that storm-wave action and currents have a strong control on sand-bar formation.

Because the shelf is sediment starved, medium to coarse sand only dominates in nearshore sediments (as revealed from the sediment analysis; Figs 7, 8). Farther north (i.e. in front of Capel River mouth) it is likely that finer sediment is kept in suspension above the seabed where waves and currents sweep it towards the southern part of the bay. Here, due to a combination of coastal morphology, seagrass and hydrodynamic controls, the sediment is rearranged in linear sandbars, oblique to the coastline. This phenomenon has been described from several regions around the world, including North Carolina (United States of America. Murray & Thieler 2004) and New Zealand (Green *et al*. 2004) where longshore currents and large waves deposit coarse material on the seafloor.

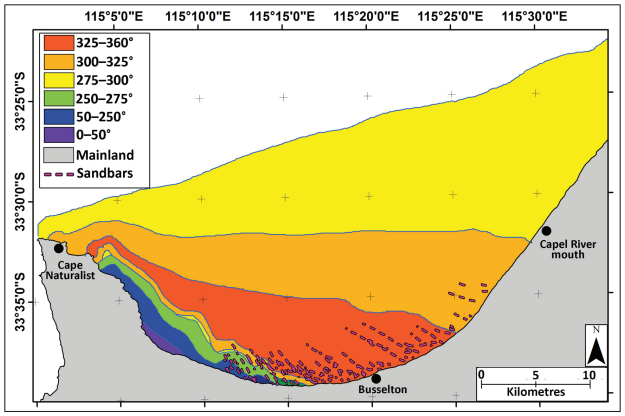

Figure 11. Predicted mean wave direction during storm events (redrawn after Pattiaratchi & Wijeratne 2011) with superimposed sandbar tracks. Note that the sandbar crests rotate according to the prevalent wave direction.

Palaeochannels

Surficial and buried incisions have been described in detail in several studies worldwide, using different methods, including bathymetric and seismic data. Ryan *et al*. (2007), for example, employed various bathymetric datasets to detect several palaeochannels between the Burdekin and Fitzroy Rivers (north-eastern Australia). Bufarale *et al*. (2017) mapped three sets of palaeochannels under the modern Swan River (adjacent to Perth central business district, Western Australia) using a boomer system. Similarly, underwater seismic refraction was employed by Whiteley & Stewart (2008) to identify a major palaeochannel under the modern Lane Cove River (Sydney, New South Wales). McNinch and collaborators (McNinch 2004; Browder & McNinch 2006; Schupp *et al*. 2006; McNinch & Miselis 2012; Thieler *et al*. 2014) have described buried palaeochannels and oblique sandbars, along North Carolina and Virginia (U.S. central Atlantic coast) using seismic profiles, combined with swath bathymetry and side-scan sonar images.

Within the study area, several surficial and buried palaeochannels have been detected through high-resolution bathymetric and seismic datasets. Buried palaeochannels are mainly found in A1, where six incisions can be depicted in the seismic profiles (Fig. 10). In A2 and A3, four and three main buried palaeochannels can be recognised, respectively. In area A2, the westernmost buried palaeochannels appear to be the prolongation of channel 1 and 2 (Fig. 10) seaward. In Area 3, a deep incision is clearly observed in the seismic profiles close to the shoreline (Fig. 2). The palaeochannel is directly in line with the modern mouth of the Capel River, evidence that an ancient Capel River was active also in the past. At present, the incision is ~5 m deep, but considering that erosion of the upper part of the unit is likely to have happened, this channel and related palaeoriver might have been more significant, in terms of dimensions, discharge and flow than the modern one. The buried and surficial palaeochannels typically follow the same course, indicating that the pre-existing topography may have shaped and influenced successive morphological features (Fig. 12).

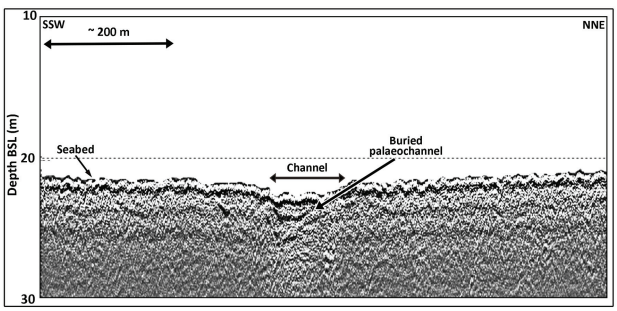

Figure 12. Seismic profile in A2 (for location see Figure 8) showing an underlying seafloor palaeochannel that is the surficial expression of a buried incision. The vertical axis corresponds to the depth below sea level (BSL) and the scale is in metres. The sound velocity in the sediments is equivalent to ~2000 m/s.

Surficial incisions, recognisable in the high-resolution bathymetric composite images, are more numerous in Area 3. The discrepancy is attributable to different Holocene thicknesses between the north-eastern A3 and the south-western A1. In the latter, where the Holocene unit is well-developed and a large amount of sediment is trapped along the sandbars, the palaeochannels have been infilled and covered up, and hence not recognisable within the bathymetric data, only in seismic profiles (Fig. 13). In A3, on the other hand, strong coastal currents (Fahrner & Pattiaratchi 1994) and the lack of seagrass meadows (McMahon *et al*. 1997; Oldham *et al*. 2010) have limited the deposition of sediment that instead has been transported and deposited farther south, leaving the surficial incisions more evident in the bathymetric data.

In central-western Geographe Bay (near study area A1), similar to along the coasts of North Carolina and Virginia (U.S.A.; Browder & McNinch 2006) and Paraná inner shelf (southern Brazil; Oliveira 2015), buried palaeochannels and oblique sandbars are found adjacent (Fig. 13). However, unlike coastal U.S.A. and Brazil, where palaeochannels have been argued to influence the development of shore-oblique sandbars (McNinch 2004), in Geographe Bay this relationship is not significant as hydrodynamic conditions (waves and currents) are the main process involved in the formation of bottom geomorphology (Paul & Searle 1978; Hamilton & Collins 1997; Oldham *et al*. 2010; Pattiaratchi & Wijeratne 2011).

Submerged low-relief ridges

As noted using the high-resolution bathymetric composite images, and also from the seismic profiles, small ridges can be recognised, corrugating the seafloor, near the coastline and into deeper water. The ridge complexes are topped by a veneer of Holocene deposits (especially thin in deep-water and toward the northern portion of the study area, near A2 and A3, respectively). The cores of the ridges are inferred to be composed of Tamala Limestone (Ramsey *et al*. 2016).

Shore parallel ridges are common structures along the Western Australian coast, both onshore (Commander 2003) and submerged on the shelf (James *et al*. 1999; Twiggs & Collins 2010; Brooke *et al*. 2010, 2014; Nichol & Brooke 2011), recording major past sea level changes. These geomorphological structures are relict landforms, like shoreface palaeodunes or beach ridges, which are commonly found in carbonate-dominated, sediment-starved coasts (Reading 2009; Brooke *et al*. 2010) and record relatively stable episodes of regressive shoreline conditions, followed by transgressive erosion. Because of their low relief above the seabed and discontinuity, it is unlikely that these ridges have acted as a barrier inhibiting or trapping onshore sediment transport.

Similar to the onshore Swan Coastal Plain, where sub-aerial coastal dune ridges become progressively younger from east to west (Commander 2003), the submerged ridges also young in the same direction, recording Late Pleistocene relatively high sea level stages. The schematic cross sections illustrating the Late Quaternary geomorphological evolution (Fig. 14) show how shallow-water ridges in the south (area A1 in Fig. 1) might have been eroded completely or covered by Holocene sediments, whereas they are preserved in the north (area A3 in Fig. 1).The shallow-water ridges in the south (area A1) might have been eroded completely or covered by Holocene sediments.

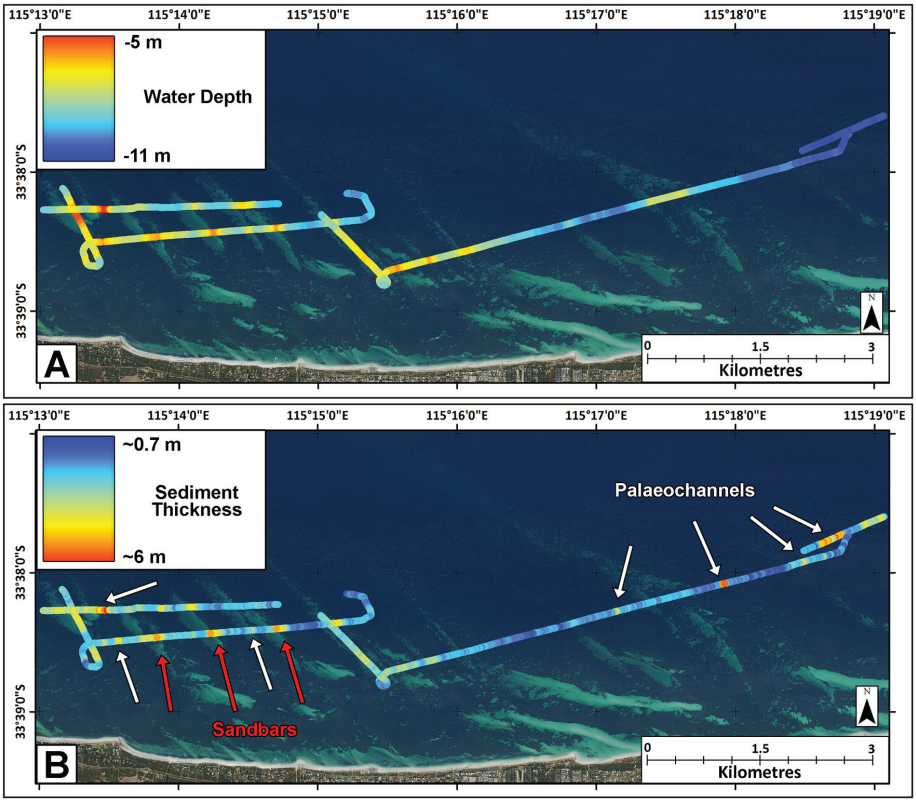

Figure 13. Water depth and Unit H sediment thickness in Area 1. Orthophoto is from SLIP Enabler portal, Landgate Imagery (Busselton Shire Jan 2016 Mosaic). A) The water depth is shallower along the oblique sand bars and deepens eastward. The water depth is in metres and calculated approximating the sound velocity of 1500 m/s. B). The Holocene unit is very thin in deeper water and between the sandbars. The sediment thickness values are expressed in metres, calculated approximating the sound velocity of 2000 m/s. The thickest sediment is found along the sandbars (red arrows) and palaeochannels (white arrows).

The shallow-water ridges were the first ridge complex to form. At the termination of MIS 5e, when the sea level was about 8 to 10 m lower than the present (Chappell *et al*. 1996), these barriers started their development, close to the innermost palaeo shoreline (Fig. 14, ~120 ka). When the sea level further dropped, stranding these features, cementation commenced. Similarly, the second ridge complex (deep-water ridges) established its shape in an analogous manner, when the sea level was 20–30 m below present (Chappell *et al*. 1996; Creveling *et al*. 2017; Fig. 14, ~100 ky). Until ~10 ky BP, most of the inner shelf was exposed, favouring the cementation of the ridges. When the sea level inundated the shelf (early Holocene), erosion took place, leaving the lithified ridges asymmetric, with a flat top (Fig. 14, present).

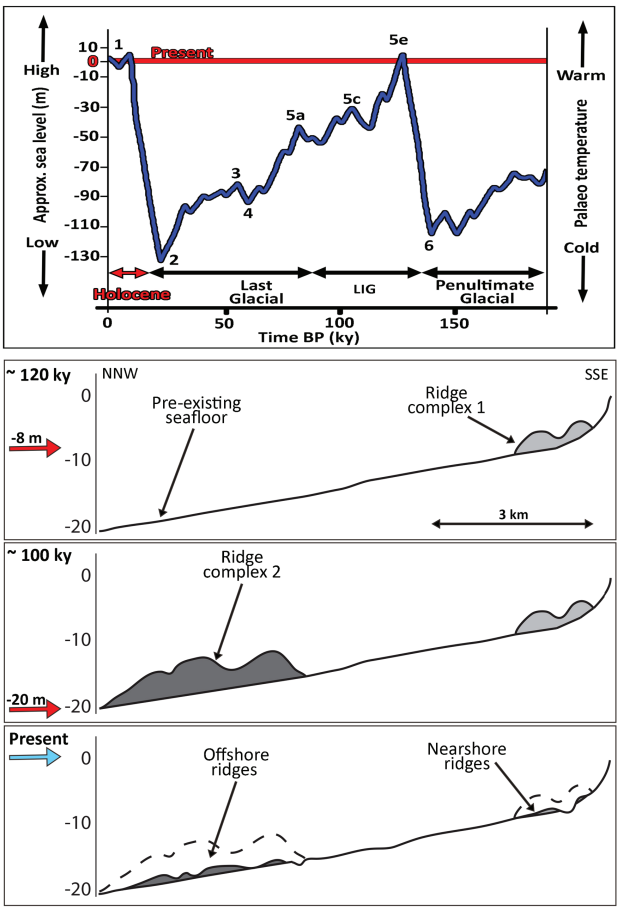

Figure 14. Top: Sea level curve since ~200 ky. Odd numbers refer to Interglacial Marine Isotope Stages (MIS) and even numbers indicate the Glacial MIS. The curve is based on oxygen isotope ratio $\delta^{18}O$ (modified after Saqab & Bourget 2015 and Bufarale *et al*. 2017). Bottom: Schematic model showing the onset and evolution of regressive beach ridges and, possibly sub-littoral deposits. The profile is a simplified cross section, near A3 in the northern portion of the study area. Horizontal axis: ~9 km; vertical axis: depth values are in metres, referred to the present sea level (where 0 corresponds to modern mean sea level). The arrows represent the stage of sea level, in different time; red: falling sea level, blue: rising sea level. The figure has been drawn based on the data from this study and the conceptual model proposed by Brooke *et al*. (2010) and Brooke *et al*. (2014).

The chronostratigraphic interpretation of these geomorphic features is supported by several studies carried out on similar structures along the state's coast, in particular in the South West (notably Brooke *et al*. 2010, 2014). These studies describe the chronology and the nature of three submerged ridge sets, between Rottnest Island and Cockburn Sound, from nearshore up to 50–60 m of depth BSL. In the present study the two shallow ridges are equivalent to the shallow-water and deep-water features and the third set, not included in this investigation, is more recent (MIS 5a). Nevertheless, additional coring and dating of both the ridge complexes could help to confirm this interpretation, and also provide a better assessment of the late Pleistocene evolution of the South West coast.

CONCLUSIONS

Reflection seismic data, combined with high-resolution composite bathymetric datasets and sedimentological analysis, provided the following new insights into the inner continental shelf in Geographe Bay:

1) Shallow architecture and stratigraphy is revealed for the first time. The seismic profiles show three main sedimentary units, separated by unconformities and deposited under various sea level conditions, which include:
   - An acoustic basement (TB, Leederville Formation), dated as Early Cretaceous;
   - One intermediate unit (TP), belonging to Tamala Limestone, of mid- to late Pleistocene age;
   - A surficial unit (TH), deposited since the early Holocene, at around 10 ky.
2) The surficial sediment of the Holocene unit is dominated by quartz but also include a percentage of carbonates and other accessory minerals and rock fragments. Finer siliciclastic sediment is more dominant on top of topographic highs and sandbars. Coarse and very coarse material, mainly carbonate, tends to accumulate in the swales and depressions. These Holocene deposits are hence the result of a combination of erosion of older formations (mainly Tamala Limestone, although heavy minerals derive from the erosion of the Leederville Formation) and *in situ* accumulation of carbonate sediment from seagrass and other benthic communities.
3) Three main features that characterise the seabed are:
   - Several palaeochannels (buried and surficial) that are an expression of previous sea-level lowstands.
   - Near-continuous, asymmetrical sandbars and associated swales, that extend obliquely from nearshore to ~6 km seaward. These linear features mostly lie in the south-western portion of the bay, and generally have an almost bare stoss flank and a lee side intensely colonised by seagrass. The sandbars result from (a) local hydrodynamics, causing the sandbars to be primary sediment sinks of siliciclastic grains, with waves and currents (including longshore)

influencing the geomorphology in the inner continental shelf; (b) grain size and (c) the influence of seagrass meadows.

- Two sets of shore-parallel, low-relief ridges, at depths of <10 m and ~20 m, represent relict landforms, probably regressive beach ridges and sub-littoral deposits (paleo-dunes), belonging to the Tamala Limestone. These late Pleistocene geomorphological structures formed during relatively high sea-level stages (end of MIS 5e – start of MIS 5d and 5c, respectively). The ridges were subsequently cemented and subject to successive marine (transgressive) erosion. Based on the morphology of these submerged strand plains, an abrasion surface characterises the top of the ridges, where the top has been cut out, exposing the core or the base of the ridges.

The data confirm that the shelf is essentially sediment-starved and the very limited Holocene deposits produced along the shelf, have then been reworked and transported onshore by waves. In terms of sediment-resource potential, the sandbars are a reservoir of the sediment on the shelf, with the core likely to be quartz sand.

ACKNOWLEDGEMENTS

The authors would like to acknowledge the DoT (Fremantle, Western Australia) for providing the hydrographic survey vessel and the bathymetric data. In particular thanks are extended to Kim Edwards, skipper of the hydrographic survey vessel *Alec Hansen III* and Karl Ilich. Additional funding was provided by a University of Western Australia's Research Collaboration Award. Many thanks to John Gann and Steve Cutcomb (Chesapeake Technology, Inc.) and Giovanni De Vita for their technical support. Alexandra Stevens is acknowledged for critically reviewing the manuscript. The journal editors are acknowledged for their careful revisions. GB acknowledges the contribution of an Australian Government Research Training Program Scholarship in supporting this research and the support provided by the Society for Underwater Technology (SUT) through the SUT Chris Lawlor 2016 Scholarship.

REFERENCES

Baker R G V & Haworth R J 1997. Further evidence from relic shellcrust sequences for a late Holocene higher sea level for eastern Australia. *Marine Geology* **141**, 1–9.

Baker R G V & Haworth R J 2000. Smooth or oscillating late Holocene sea-level curve? Evidence from the palaeo-zoology of fixed biological indicators in east Australia and beyond. *Marine Geology* **163**, 367–386.

Baker R G V, Haworth R J & Flood P G 2001. Inter-tidal fixed indicators of former Holocene sea levels in Australia: a summary of sites and a review of methods and models. *Quaternary International* **83–85**, 257–273

Baker R G, Haworth R J & Flood P G 2005. An oscillating Holocene sea level? Revisiting Rottnest Island, Western Australia, and the Fairbridge eustatic hypothesis. *Journal of Coastal Research* **42**, 3–14.

Barr S & Eliot M 2011. Busselton coastal protection *in* Coasts and Ports 2011: Diverse and Developing: Proceedings of the 20th Australasian Coastal and Ocean Engineering Conference and the 13th Australasian Port and Harbour Conference (p. 30). *Engineers Australia.*

Barr S A, Staples O, Eliot I, Darby O, Abrahamse D & Stul T 2017. Adaptation to coastal inundation in a low lying, highly dynamic regional area. *Australasian Coasts & Ports* 2017: Working with Nature, **1037**.

Bianchi C & Gersonde R 2002. The Southern Ocean surface between Marine Isotope Stages 6 and 5d: Shape and timing of climate changes. *Palaeogeography, Palaeoclimatology, Palaeoecology* **187**, 151–177.

Brooke B, Creasey J & Sexton M 2010. Broad-scale geomorphology and benthic habitats of the Perth coastal plain and Rottnest Shelf, Western Australia, identified in a merged topographic and bathymetric digital relief model. *International Journal of Remote Sensing* **31**, 6223–6237.

Brooke B P, Olley J M, Pietsch T, Playford P E, Haines P W, Murray-Wallace C V & Woodroffe C D 2014. Chronology of Quaternary coastal aeolianite deposition and the drowned shorelines of southwestern Western Australia – a reappraisal. *Quaternary Science Reviews* **93**, 106–124.

Brooke B P, Nichol S L, Huang Z & Beaman R J 2017. Palaeoshorelines on the Australian continental shelf: Morphology, sea-level relationship and applications to environmental management and archaeology. *Continental Shelf Research* **134**, 26–38.

Browder A G & McNinch J E 2006. Linking framework geology and nearshore morphology: correlation of paleo-channels with shore-oblique sandbars and gravel outcrops. *Marine Geology* **231**, 141–162.

Bufarale G & Collins L B 2015. Stratigraphic architecture and evolution of a barrier seagrass bank in the mid-late Holocene, Shark Bay, Australia. *Marine Geology* **359**, 1–21.

Bufarale G, O'Leary M, Stevens A & Collins L B 2017. Sea level controls on palaeochannel development within the Swan River estuary during the Late Pleistocene to Holocene. *Catena* **153**, 31–142.

Bureau of Meteorology - Australia 2011. Climate summary statistics Busselton Shire. http://www.bom.gov.au/climate/averages/tables/cw_009515.shtml

Carrigy M A & Fairbridge R W 1954, Recent sedimentation, physiography and structure of the continental shelves of Western Australia. *Journal of the Royal Society of Western Australia* **38**, 65–95.

Chappell J, Omura A, Esat T, McCulloch M, Pandolfi J, Ota Y & Pillans B 1996. Reconciliation of late Quaternary sea levels derived from coral terraces at Huon Peninsula with deep sea oxygen isotope records. *Earth and Planetary Science Letters* **141**, 227–236.

Chiarella D, Longhitano S G, Sabato L & Tropeano M 2012. Sedimentology and hydrodynamics of mixed (siliciclastic-bioclastic) shallow-marine deposits of Acerenza (Pliocene, Southern Apennines, Italy). *Italian journal of geosciences* **131**, 136–151.

Coastal Information, Department of Transport 2016. https://catalogue.data.wa.gov.au/dataset/composite-surfaces-multibeam-lidar-laser (valid at: 22/06/2017)

Cockbain A E & Playford P E 1973. Stratigraphic nomenclature of Cretaceous rocks in the Perth Basin: Western Australia *Geological Survey of Western Australia Annual Report* **1972**, 26–31.

Collins L B & Baxter J L 1984. Heavy mineral–bearing strandline deposits associated with high-energy beach environments, southern Perth Basin, Western Australia. *Australian Journal of Earth Sciences* **31**, 287–292.

Collins L B 1988. Sediments and history of the Rottnest Shelf, southwest Australia: a swell-dominated, non-tropical carbonate margin. *Sedimentary Geology* **60**, 15–49.

Collins L B, Zhao J X & Freeman H 2006. A high-precision record of mid–late Holocene sea level events from emergent coral pavements in the Houtman Abrolhos Islands, southwest Australia. *Quaternary International* **145**, 78–85.

Commander D P 1982. The Bunbury shallow drilling groundwater investigation. *Western Australia Geological Survey*, 32–52.

Commander P 2003. Outline of the geology of the Perth region. *Australian Geomechanics Journal* **38**, 7–16.

Creveling J R, Mitrovica J X, Clark P U, Waelbroeck C & Pico T 2017. Predicted bounds on peak global mean sea level during marine isotope stages 5a and 5c. *Quaternary Science Reviews* **163**, 193–208.

CSIRO 2015. Tidal Dataset - CAMRIS - Maximum Tidal Range. v1. CSIRO. Data Collection. http://doi.org/10.4225/08/551485767777F

Deeney A C 1989. Geology and groundwater resources of the superficial formations between Pinjarra and Bunbury, Perth Basin. *Geological Survey of Western Australia* **26**, 31–57.

Department of Water. Surface Water Hydrology Series Report no. 24 2008. https://www.water.wa.gov.au/__data/assets/pdf_file/0019/2575/81757.pdf (valid at: 19/04/2018).

Duncan A J, Gavrilov A & Li F 2009. Acoustic propagation over limestone seabeds. In *Proceedings of Acoustics*: Research to Consulting, Annual Conference of the Australian Acoustical Society, 1–6.

Fahrner C K & Pattiaratchi C B 1994. The physical oceanography of Geographe Bay, Western Australia. Report prepared for the Water Authority of Western Australia.

Fairbridge R W 1961. Eustatic changes in sea level. *Physics and Chemistry of the Earth* **4**, 99–185.

Geographe Catchment Council 2008. Geographe Catchment Management Strategy. A Report for the Geographe Catchment Council, Water and Rivers Commission and National Heritage Trust.

Gozzard J R 2007. A reinterpretation of the Guildford formation. *Australian Geomechanics Journal* **42**, 59–79.

Green M O, Vincent C E & Trembanis A C 2004. Suspension of coarse and fine sand on a wave-dominated shoreface, with implications for the developments of rippled scour depressions. *Continental Shelf Research* **24**, 317–335.

Hamilton N T M & Collins L B 1997. Morphostratigraphy and evolution of a Holocene composite barrier at Minninup, southwestern Australia. *Australian Journal of Earth Sciences* **44**, 113–124.

Hearty P J 2003. Stratigraphy and timing of eolianite deposition on Rottnest Island, Western Australia. *Quaternary Research* **60**, 211–222.

Hearty P J, Hollin J T, Neumann A C, O'leary M J & McCulloch M 2007. Global sea-level fluctuations during the Last Interglaciation (MIS 5e). *Quaternary Science Reviews* **26**, 2090–2112.

Hirschberg K-J B 1988. Busselton Shallow Drilling Project Bore Completion Reports. *Geological Survey of Western Australia*, Hydrogeology Report No. 1988/**17**, 17–25.

Hirschberg K-J B 1989. Busselton shallow-drilling groundwater investigation, Perth Basin. *Geological Survey of Western Australia*, Professional Papers, Report **25**, 7–37.

Jahnert R J & Collins L B 2013. Controls on microbial activity and tidal flat evolution in Shark Bay, Western Australia. *Sedimentology* **60**, 1071–1099.

James N P, Collins L B, Bone Y & Hallock P 1999. Subtropical carbonates in a temperate realm: modern sediments on the southwest Australian shelf. *Journal of Sedimentary Research* **69**, 1297–1321.

James N P & Bone Y 2010. *Neritic carbonate sediments in a temperate realm: southern Australia*. Springer Science & Business Media, 254.

Kearey P, Brooks M & Hill I 2002. *An introduction to geophysical exploration.* Third edition, Blackwell Scientific, Oxford, UK.

Kendrick G W, Wyrwoll K-H & Szabo B J 1991. Pliocene-Pleistocene coastal events and history along the western margin of Australia. *Quaternary Science Reviews* **10**, 419–439.

Lambeck K & Chappell J 2001. Sea level change through the last glacial cycle. *Science* **292,** 679–686.

Lambeck K, Esat Tm & Potter E-K 2002. Links between climate and sea levels for the past three million years. *Nature* **419**, 199–206.

Lipar M & Webb J A 2014. Middle–late Pleistocene and Holocene chronostratigraphy and climate history of the Tamala Limestone, Cooloongup and Safety Bay Sands, Nambung National Park, southwestern Western Australia. *Australian Journal of Earth Sciences* **61,** 1023–1039.

Longhitano S G 2011. The record of tidal cycles in mixed silici–bioclastic deposits: examples from small Plio–Pleistocene peripheral basins of the microtidal Central Mediterranean Sea. *Sedimentology* **58**, 691–719.

McMahon K, Young E, Montgomery S, Cosgrove J, Wilshaw J & Walker D I 1997. Status of a shallow seagrass system, Geographe Bay, south-western Australia. *Journal of the Royal Society of Western Australia Royal* **80**, 255–262.

McMahon T A & Finlayson B L 2003. Droughts and anti-droughts: the low flow hydrology of Australian rivers. *Freshwater Biology* **48,** 1147–1160.

McNinch J E 2004. Geologic control in the nearshore: shore-oblique sandbars and shoreline erosional hotspots, Mid-Atlantic Bight, USA. *Marine Geology* **211**, 121–141.

McNinch J E & Miselis J L 2012. Geology metrics for predicting shoreline change using seabed and sub-bottom observations from the surf zone and nearshore. *International Association of Sedimentologists Special Publication* **44**, 99–120.

Munsell A H 1954. *Munsell soil color chart.* U.S. Dept. Agriculture Soil Survey Manual

Murray A B & Thieler E R 2004. A new hypothesis and exploratory model for the formation of large-scale inner-shelf sediment sorting and "rippled scour depressions". *Continental Shelf Research* **24**, 295–315.

Murray-Wallace C V & Kimber R W L 1989. Quaternary marine aminostratigraphy: Perth Basin, Western Australia. *Australian Journal of Earth Sciences* **36**, 553–568.

Nichol S L & Brooke B P 2011. Shelf habitat distribution as a legacy of Late Quaternary marine transgressions: a case study from a tropical carbonate province. *Continental Shelf Research* **31**, 1845–1857.

Oldham C, Lavery P, McMahon K, Pattiaratchi C & Chiffings T 2010. Seagrass wrack dynamics in Geographe Bay, Western Australia. Report to Western Australian Department of Transport, and Shire of Busselton.

Oliveira L H S D 2015. Morfologia e sedimentologia da plataforma continental interna paranaense. Doctoral Thesis. Universidade Federal do Paraná, Setor de Ciências da Terra, Programa de Pós-Graduação em Geologia. https://educapes.capes.gov.br/handle/1884/39930 (May 2017).

Pattiaratchi C & Wijeratne S 2011. Port Geographe sand and seagrass wrack modelling study, Western Australia. Report prepared for Department of Transport (WA). SESE report no. 465, School of Environmental Systems Engineering, the University of Western Australia, Perth.

Pattiaratchi C B, Wijeratne E M S & Bosserelle C 2011. Sand and seagrass wrack modelling in Port Geographe, south-western Australia. *Proceedings of Coasts and Ports 2011*, Engineers Australia.

Pattiaratchi C B, Wijeratne E M S, Roncevich L & Holder J 2015. Interaction between seagrass wrack and coastal structures: lessons from Port Geographe, southwestern Australia. *Proceedings of Coasts and Ports 2015,* Engineer Australia.

Pattiaratchi C B, Wijeratne S, Roncevich L & Holder J 2017. The influence of nearshore sandbars on coastal stability in port geographe, South-west Australia. *Australasian Coasts & Ports 2017: Working with Nature*, p.865.

Paul M J & Searle J D 1978. Shoreline Movements Geographe Bay Western Australia *in*: Fourth Australian Conference on

Coastal and Ocean Engineering: *Managing the Coast*. Barton, A.C.T.: Institution of Engineers, Australia.

Playford P E, Cockbain A E & Lowe G H 1976. Geology of the Perth Basin. *Geological Survey of Western Australia Bulletin* **124**.

Playford P E 1997. Geology and hydrogeology of Rottnest Island, Western Australia. Pages: 783–810 *in* Vacher L H & Quinn T M, editors *Geology and Hydrogeology of Carbonate Islands, Developments in Sedimentology*, Elsevier, Amsterdam.

Price D M, Brooke B P & Woodroffe C D 2001. Thermoluminescence dating of eolianites from Lord Howe Island and south-west Western Australia. *Quaternary Science Reviews* **20**, 841–846.

Probert D H 1967. Groundwater in the Busselton Area: Progress Report on Exploratory Drilling. *Geological Survey of Western Australia*.

Ramsay P, Miller W & Murrell D. 2016. Supporting renewable energy projects using high resolution hydrographic and geophysical survey techniques, Garden Island, Western Australia. *Underwater Technology* **33**, 229–237.

Reading H G 2009. *Sedimentary environments: processes, facies and stratigraphy*. John Wiley & Sons.

Ryan D A, Bostock H C, Brooke B P & Marshall J F 2007. Bathymetric expression of the Fitzroy River palaeochannel, northeast Australia: Response of a major river to sea level change on a semi-rimmed, mixed siliciclastic-carbonate shelf. *Sedimentary Geology* **201**, 196–211.

Saqab M M & Bourget J 2015. Controls on the distribution and growth of isolated carbonate build-ups in the Timor Sea (NW Australia) during the Quaternary. Mar. *Petroleum Geology* **62**, 123–143. doi:10.1016/j.marpetgeo.2015.01.014.

Schafer D, Johnson S & Kern A 2008. Hydrogeology of the Leederville aquifer in the western Busselton-Capel Groundwater Area. Department of Water Hydrogeological record series **HG31**.

Schupp C A, McNinch J E & List J H 2006. Nearshore shore-oblique bars, gravel outcrops, and their correlation to shoreline change. *Marine Geology* **233**, 63–79.

Skene D, Ryan D, Brooke B, Smith J & Radke L 2005. The geomorphology and sediments of Cockburn Sound. *Geoscience Australia*, Record **2005/10**, 88

Stirling C H, Esat T M, McCulloch M T & Lambeck K 1995. High-precision U-series dating of corals from Western Australia and implications for the timing and duration of the Last Interglacial. *Earth and Planetary Science Letters* **135**, 115–130.

Szabo B J 1979. Uranium-series age of coral reef growth on Rottnest Island, Western Australia. *Marine Geology* **29**, M11–M15.

Thieler E R, Foster D S, Himmelstoss E A & Mallinson D J 2014. Geologic framework of the northern North Carolina, USA inner continental shelf and its influence on coastal evolution. *Marine Geology* **348**, 113–130.

Twiggs E J & Collins L B 2010. Development and demise of a fringing coral reef during Holocene environmental change, eastern Ningaloo Reef, Western Australia. *Marine Geology* **275**, 20–36.

Van Niel K P, Holmes K W & Radford B 2009. Seagrass Mapping Geographe Bay 2004–2007. Report prepared for: Southwest Catchment Council, 25 pp, University of Western Australia.

Wharton P H 1981. The geology and hydrogeology of the Quindalup borehole line. *Western Australia Geological Survey, Annual Report* for 1980, 27–34.

Wharton P H 1982. The geology and hydrogeology of the Quindalup borehole line in Southern Perth Basin, Western Australia. *Western Australia Geological Survey*, Record **1982/2**.

White K & Comer S 1999. Capel River action plan. Geographe Catchment Council -Geocatch and the Capel Land Conservation District Committee.

Whitehouse J 2007. Evaluation of mineral resources of the continental shelf, New South Wales. *New South Wales Geological Survey*, Quarterly Notes **124**, 23.

Whiteley R J & Stewart S B 2008. Case studies of shallow marine investigations in Australia with advanced underwater seismic refraction (USR). Exploration Geophysics **39**, 34–40.